Characterization of Dental Pulp Myofibroblasts in Rat Molars after Pulpotomy

Naoki Edanami, DDS, Nagako Yoshiba, DDS, PhD, Naoto Ohkura, DDS, PhD, Ryosuke Takeuchi, DDS, Aiko Tohma, DDS, Yuichiro Noiri, DDS, PhD and Kunihiko Yoshiba, DDS, PhD

Division of Cariology, Operative Dentistry and Endodontics, Department of Oral Health Science, Course for Oral Life Science, Niigata University Graduate School of Medical and Dental Sciences, Niigata, Japan

Corresponding author: Kunihiko Yoshiba,

Division of Cariology, Operative Dentistry and Endodontics

Department of Oral Health Science, Course for Oral Life Science

Niigata University Graduate School of Medical and Dental Sciences

2-5274 Gakkocho-dori, Chuo-ku, Niigata 951-8514, Japan.

Phone: +81-25-227-2865; Fax: +81-25-227-2864

E-mail: yoshiba@dent.niigata-u.ac.jp

Abstract

Introduction

Myofibroblasts express α-smooth muscle actin (α-SMA) and play a critical role in wound healing. Myofibroblast differentiation is controlled by the joint actions of transforming growth factor (TGF)-β1 and the extradomain A fibronectin splice variant (EDA-FN). Currently, the contribution of myofibroblasts to dental pulp healing is unknown. Therefore, we analyzed expressional characteristics of α-SMA-positive cells and investigated TGF-β1, EDA-FN, and α-SMA expression levels after pulpotomy to better understand dental pulp healing.

Methods

The maxillary first molars of 8-week-old Wistar rats were pulpotomized with mineral trioxide aggregate. After 1-14 days, localization and co-localization of α-SMA, RECA-1 (as a marker of endothelial cells), NG2 (as a marker of perivascular cells), prolyl-4-hydroxylase (P4H; as an additional marker of myofibroblasts), and EDA-FN were analyzed using immunohistochemistry and double-immunofluorescence. Time-course changes in the mRNA expression levels of TGF-β1, EDA-FN, and α-SMA were evaluated using quantitative RT-PCR analysis.

Results

Spindle-shaped α-SMA-positive cells transiently appeared following pulpotomy. These cells initially emerged in the pulp core at day 3, then accumulated at the wound site by day 5. These cells were isolated from RECA-1-positive cells, and did not express NG2 but did express P4H. The mRNA levels of TGF-β1, EDA-FN, and α-SMA were significantly upregulated following pulpotomy. EDA-FN and α-SMA were co-localized at wound sites at day 5.

Conclusions

In association with upregulation of TGF-β1 and EDA-FN expression, α-SMA and P4H double-positive cells accumulated at wound sites following pulpotomy. This suggests that myofibroblasts participate in dental pulp healing.

Keywords: dental pulp healing, myofibroblast, α-smooth muscle actin, transforming growth factor-β1, extradomain A fibronectin splice variant

Introduction

Granulation tissue formation and extracellular matrix (ECM) reorganization are fundamental processes in wound healing. Myofibroblasts, which are typically characterized by the expression of α-smooth muscle actin (α-SMA), play a critical role in wound healing by secreting numerous cytokines and growth factors, ECM components, and ECM-degrading enzymes (1).

Dental pulp is a soft connective tissue enclosed by mineralized dentin. When the dentin barrier is disrupted by caries or traumatic injury, the dental pulp is exposed to the external environment. The application of pulp-capping materials allows coverage of the exposed site by a reparative mineralized matrix (a dentin bridge), which is generated by newly-differentiated odontoblast-like cells (2). Mineral trioxide aggregate (MTA), a calcium silicate-based cement, is regarded as the superior material for pulp capping because of its favorable potential to induce hard tissue repair (3).

In the process of dentin bridge formation, new collagenous matrix layer and spindle-shaped fibroblastic cells with well-developed cytological organization are recognized beneath dental pulp exposure sites prior to mineralized matrix formation (4, 5). Our previous study of human teeth revealed that α-SMA-positive cells transiently appeared along dental pulp wound margins (6). Although myofibroblasts are suspected to contribute to the healing of injured dental pulp, little is known regarding the characteristics of these α-SMA-positive cells.

The expression of α-SMA is the most common definition of myofibroblasts. However, there are potential limitations of using α-SMA alone to identify myofibroblasts, because vascular smooth muscle cells and pericytes also express α-SMA (7). Prolyl-4-hydroxylase (P4H), a collagen maturation enzyme, has also been suggested as a marker for activated fibroblasts and myofibroblasts (8, 9). Therefore, the co-expression of α-SMA and P4H may more robustly identify myofibroblasts.

Myofibroblast differentiation is controlled by the joint actions of transforming growth factor (TGF)-β1 and the extradomain A fibronectin splice variant (EDA-FN) (7, 10). Previous studies have highlighted the importance of TGF-β1 for α-SMA expression by dental pulp cells *in vitro* (11, 12). However, whether an association between TGF-β1 expression and myofibroblast differentiation exists *in vivo* is presently unknown. Furthermore, EDA-FN expression has not previously been investigated in dental pulp wound healing.

To better understand the contribution of myofibroblasts in dental pulp wound healing, we analyzed the histological localization and expressional characteristics of α-SMA-positive cells by immunohistochemical and double-immunofluorescence staining of rat molar pulps after pulpotomy with MTA. We further analyzed time-course changes in the expression of TGF-β1, EDA-FN and α-SMA in dental pulp wound healing by quantitative RT-PCR and immunohistochemistry.

Materials and Methods

Pulpotomy Procedures

All experiments were reviewed by the Committee on the Guidelines for Animal Experimentation of Niigata University and performed according to the recommendations of the institutional review board.

Forty-four 8-week-old Wistar rats were used. Under anesthesia by intraperitoneal injection of 8% chloral hydrate, the dental pulp of the upper left first molar was exposed at the occlusal surface, and coronal pulp tissue was removed with a #1 round carbide bur (diameter = 0.8 mm). The exposed area was rinsed with 5% sodium hypochlorite and 3% hydrogen peroxide followed by sterile saline. Hemorrhage was controlled with sterile cotton pellets. MTA (White ProRoot MTA; Dentsply Tulsa Dental, Tulsa, OK) was mixed according to the manufacturer's instructions and placed over the pulp stump. The cavity was then sealed with a flowable composite resin (Beautifil Flow; Shofu, Kyoto, Japan).

Tissue Preparation for Immunohistochemistry

Observations were made at 1, 3, 5, 7, and 14 days after the operation (1, 5, 7, 14 days: n = 4 each for sagittal sections; 3 days: n = 8 for sagittal and horizontal sections). After transcardiac perfusion of periodate-lysine-paraformaldehyde fixative following intraperitoneal anesthesia with chloral hydrate, the relevant teeth were removed together with the surrounding tissue and immersed in periodate-lysine-paraformaldehyde for an additional 24 h. Following demineralization in a 10% EDTA solution, samples were embedded in optimal cutting temperature compound (O.C.T. Compound; Sakura, Tokyo, Japan). Frozen sections were cut at a thickness of 10 μm. Horizontal sections were obtained from the upper one-third of radicular pulp.

Immunohistochemistry and Double-immunofluorescence

Primary antibodies are shown in Table 1. Sections were heat pretreated in 10 mmol/L citric acid buffer (pH = 6.0). For single immunoperoxidase staining, sections were treated with 0.3% hydrogen peroxide in phosphate-buffered saline (PBS) for 30 min, and then incubated with primary antibodies against α-SMA or EDA-FN for 2 h. After that, sections were reacted with biotinylated horse anti-mouse IgG (Vector, Burlingame, CA, USA) for 1 h and then with avidin-biotin-peroxidase complex (Elite ABC Kit; Vector) for 30 min. Immunoreactivity was visualized using the DAB substrate kit (Vector) and counterstaining performed with methyl green. For double-immunofluorescence, sections were incubated with primary antibodies against RECA-1 (a marker of endothelial cells (13)), NG2 (a marker of vascular smooth muscle cells and pericytes (14)) , P4H, or EDA-FN for 2 h, followed by incubation with Alexa Fluor 488-conjugated goat anti-mouse IgG or Alexa Fluor 488-conjugated goat anti-rabbit IgG (Invitrogen, Carlsbad, CA, USA) for 1 h. Sections

were then incubated with Cy3-conjugated anti-α-SMA antibody for 2 h. All sections were washed with PBS between each incubation step. Negative control staining was performed by replacing the primary antibodies with non-immune mouse or rabbit IgG (Santa Cruz Biotechnology, Dallas, TX, USA). Control sections did not show any specific immunoreactivity.

Quantitative RT-PCR Analysis

At 1, 3, 5, 7, and 14 days after the pulp capping procedure (n = 4 each timepoint), animals were sacrificed via inhalation of an overdose of sevoflurane (Wako, Osaka, Japan). After extraction of the upper first molars, the roots were scraped using a Gracey curette. Molars were then ground to fine particles. Total RNA was isolated from the particles using an RNeasy Plus Micro kit (Qiagen, Hilden, Germany) according to the manufacturer's instructions. Quantitative RT-PCR was carried out using a One Step SYBR PrimeScript PLUS RT-PCR kit (Takara Bio, Shiga, Japan) with the Opticon Real-Time PCR System (MJ Research, Inc., Waltham, MA, USA). The sequences of the primers are shown in Table 2.Target gene mRNA expression levels were normalized to those of β-actin mRNA. Data were statistically evaluated by the Dunnett's test using statistical software (SPSS 10J for Windows, SPSS Japan, Tokyo, Japan).

Results

Histological Changes

The dental pulp of an untreated normal teeth contains an odontoblast layer, sub-odontoblastic layer, and a pulp core with a low density of cells (Fig. 1A a). At postoperative day 1, a thin degenerative layer was observed along the amputated site, with few inflammatory cells scattered beneath this layer (Fig. 1A b). At day 3, the inflammation had resolved, and some spindle-shaped cells appeared beneath the degenerative layer (Fig. 1A c). At day 5, a layer of granulation-like tissue with blood vessels was recognized at the exposure site (Fig. 1A d). A thin dentin bridge was observed at the exposure site at day 7 (Fig. 1A e). At day 14, all specimens exhibited dentin bridge formation with a tubular structure and subjacent odontoblast-like cells (Fig. 1A f).

Alteration of α-SMA Expression during Pulp Healing

All teeth exhibited similar immunohistochemical changes. In untreated normal teeth, α-SMA expression was confined to blood vessels (Fig. 1B a, a', g). No alteration in α-SMA immunostaining was observed at postoperative day 1 (Fig. 1B b). However, numerous α-SMA-positive spindle-shaped cells emerged at day 3, and these were scattered in the pulp core of radicular pulp (Fig. 1B c, c', h, h'). At day 5, α-SMA-positive spindle-shaped cells were abundant at the exposure site (Fig. 1B d, d'). Thereafter, numbers of α-SMA-positive cells were decreased by day 14 (Fig. 1B e, f, f'),

with these cells detected only along blood vessels in a similar manner to the situation of untreated teeth.

Double-immunofluorescence of α-SMA and RECA-1, NG2, or P4H

In untreated normal teeth, all α-SMA-positive cells wrapped around RECA-1-positive endothelial cells and co-expressed NG2 (data not shown). Conversely, on postoperative day 3, α-SMA-positive spindle-shaped cells were scattered in the pulp core and isolated from RECA-1-positive endothelial cells (Fig. 2A a–c). The α-SMA-positive spindle-shaped cells did not express NG2 (Fig. 2A d–f) but did express P4H (Fig. 2A g–i). At day 5, the α-SMA-positive cells detected at the exposure site also co-expressed P4H (Fig. 2 B a–d).

mRNA Expression Levels of TGF-β1, EDA-FN, and α-SMA

Compared with untreated normal teeth, the expression levels of TGF-β1 mRNA were significantly increased at postoperative days 1–3 with a peak at day 1 (Fig. 3A). The expression levels of EDA-FN mRNA were significantly increased at days 1–5 with a peak at day 1 (Fig. 3B). mRNA expression levels of α-SMA were significantly increased at days 1–7, with a peak at day 3 (Fig. 3C). Thereafter, the expressional levels of TGF-β1, EDA-FN, and α-SMA decreased to the levels present in untreated normal teeth by day 14 (Fig. 3A–C).

EDA-FN Immunohistochemistry and Double-immunofluorescence with α-SMA

Little or no immunostaining of EDA-FN was detectable in untreated normal teeth (Fig. 4A). At postoperative day 1, EDA-FN was detected particularly around blood vessels (Fig. 4B). The area of EDA-FN staining had widened by day 5 (Fig. 4C, D). At day 5, intense staining of EDA-FN was detected, especially at the exposure site (Fig. 4D). From day 7 onward, EDA-FN staining remained positive but became weaker (Fig. 4E, F). Double-immunofluorescence revealed intense EDA-FN fluorescence in the vicinity of α-SMA-positive cells at the exposure site at postoperative day 5 (Fig. 4G–I).

Discussion

Our present study reveals that α-SMA-positive cells undergo spatio-temporal alterations during dental pulp wound healing. In untreated normal pulp, α-SMA immunoreactivity was detected only in vascular smooth muscle cells and pericytes. However, spindle shaped α-SMA-positive cells transiently emerged in the pulp core at postoperative day 3. Thereafter, these cells were detected at the wound site at day 5. The α-SMA-positive cells had disappeared by day 14, at which time a dentin bridge had completely formed.

Double-immunofluorescence for α-SMA and NG2 or RECA-1 indicated that the spindle-

shaped α-SMA-positive cells were not components of the vascular wall. Meanwhile, the α-SMA-positive cells co-expressed P4H, suggesting that these cells are likely myofibroblasts. These myofibroblasts accumulated at the exposure site at postoperative day 5, at which time new dentin-like matrix had yet to form. P4H has been shown to be enriched in collagen-producing fibroblast subtypes (15). Meanwhile, lung myofibroblasts exhibit higher expression of P4H and collagen than do control fibroblasts (9). Thus, abundant collagen synthesis by myofibroblasts may facilitate ECM reorganization of the injured pulp.

Myofibroblast differentiation requires both TGF-β1 and EDA-FN. TGF-β1 initially stimulates EDA-FN deposition, with myofibroblasts then differentiating within granulation tissue (10, 16). The subcutaneous tissue of EDA-FN-null mice exhibits less collagen deposition and possesses fewer α-SMA-expressing myofibroblasts at sites of injury (17). Thus, we further analyzed time-course changes in the expression levels of TGF-β1 and EDA-FN, and evaluated whether these changes correlate with myofibroblast differentiation. The mRNA expression levels of TGF-β1 and EDA-FN were immediately increased and exhibited a peak at postoperative day 1. EDA-FN immunoreactivity was faint in untreated normal pulp, but first detected at postoperative day 1. The upregulation of TGF-β1 and EDA-FN was followed by the appearance of myofibroblasts and the peak of the mRNA expression of α-SMA at postoperative days 3. Double-immunofluorescence analysis identified intense EDA-FN immunofluorescence in the vicinity of α-SMA-positive cells below the exposure site at day 5. Taken together, these findings support the notion that myofibroblast differentiation in dental pulp healing also progresses under the influence both of TGF-β1 and EDA-FN, as previously suggested in other organs (7).

Myofibroblasts typically migrate through tissues to sites of injury in response to chemokines released at the site of injury (18). However, whether the myofibroblasts we detected in the pulp core had migrated to the injury site remains unclear. Some studies have suggested that the pulp cells of sliced-cultured teeth migrate from the pulp core to the periphery by stimulation of TGF-β1 (19). Additionally, radicular cells in rat molars may migrate from the center to the periphery, and from the root toward the crown after pulp exposure (20). Furthermore, treatment of pulp cells with MTA extracts enhances cellular migration and stress fiber assembly (21). Therefore, we suspect that the myofibroblasts that appeared in the pulp core were recruited to the wound site.

Although the origin of myofibroblasts has not been conclusively established to date (22), a recent study suggested that perivascular Gli1-expressing mesenchymal stem cells are a major cellular origin of myofibroblasts in kidney, heart, liver and lung tissues (23). In mouse incisors, Gli1-expressing periarterial cells differentiate into all dental mesenchymal derivatives (24). The myofibroblasts detected in our present study initially appeared at the pulp core, which contains major blood vessels. Therefore, these myofibroblasts may arise from Gli1-expressing cells. Meanwhile, α-SMA-positive cells have been suggested as a possible source of osteoblasts (25, 26) or odontoblast-

like cells in humans (6) and mice (27). Therefore, some myofibroblasts could be the source of newly-differentiated odontoblast like cells.

In conclusion, we have revealed the distributional alterations of α-SMA-positive cells and identified their myofibroblastic features after pulpotomy with MTA. The accumulation of myofibroblasts at the wound site suggests that myofibroblasts participates in reparative dentinogenesis. Therefore, myofibroblasts could serve as a new therapeutic target for vital pulp therapy.

Acknowledgements

This work was supported by Grants-in-Aid for Scientific Research from the Japan Society for the Promotion of Science (no. 24592863, 16H05516E to K.Y., and no. 25462952, 16K11546 to N.Y., and no. 21592417 to N.O.).

The authors deny any conflicts of interest related to this study.

References

1. Powell DW, Mifflin RC, Valentich JD, Crowe SE, Saada JI, West AB. Myofibroblasts. I. Paracrine cells important in health and disease. Am J Physiol 1999;277(1 Pt 1):C1-9.
2. Ruch J V. Odontoblast differentiation and the formation of the odontoblast layer. J Dent Res 1985;64 Spec No:489–98.
3. Okiji T, Yoshiba K. Reparative dentinogenesis induced by mineral trioxide aggregate: a review from the biological and physicochemical points of view. Int J Dent 2009;2009:464280. Doi: 10.1155/2009/464280.
4. Yoshiba K, Yoshiba N, Nakamura H, Iwaku M, Ozawa H. Immunolocalization of fibronectin during reparative dentinogenesis in human teeth after pulp capping with calcium hydroxide. J Dent Res 1996;75(8):1590–7.
5. Tziafas D, Pantelidou O, Alvanou A, Belibasakis G, Papadimitriou S. The dentinogenic effect of mineral trioxide aggregate (MTA) in short-term capping experiments. Int Endod J 2002;35(3):245–54. Doi: 10.1046/j.1365-2591.2002.00471.x.
6. Yoshiba N, Yoshiba K, Ohkura N, et al. Immunohistochemical analysis of two stem cell markers of α-smooth muscle actin and STRO-1 during wound healing of human dental pulp. Histochem Cell Biol 2012;138(4):583–92. Doi: 10.1007/s00418-012-0978-4.
7. Hinz B. Formation and Function of the Myofibroblast during Tissue Repair. J Invest Dermatol 2007;127(3):526–37. Doi: 10.1038/sj.jid.5700613.
8. Matthijs Blankesteijn W. Has the search for a marker of activated fibroblasts finally come to an end? J Mol Cell Cardiol 2015;88:120–3. Doi: 10.1016/j.yjmcc.2015.10.005.
9. Akamatsu T, Arai Y, Kosugi I, et al. Direct isolation of myofibroblasts and fibroblasts from bleomycin-injured lungs reveals their functional similarities and differences. Fibrogenesis Tissue Repair 2013;6(1):15. Doi: 10.1186/1755-1536-6-15.
10. Serini G, Ropraz P, Geinoz A, Borsi L, Zardi L, Gabbiani G. The Fibronectin Domain ED-A Is Crucial for Myofibroblastic Phenotype Induction by Transforming Growth Factor- 1998;142(3):873–81. Doi: 10.1083/jcb.142.3.873.
11. Martinez EF, Araújo VC, Sousa SO, Arana-Chavez VE. TGF-beta1 enhances the expression of alpha-smooth muscle actin in cultured human pulpal fibroblasts: immunochemical and ultrastructural analyses. J Endod 2007;33(11):1313–8. Doi: 10.1016/j.joen.2007.07.040.
12. Yoshiba N, Yoshiba K, Ohkura N, et al. Correlation between Fibrillin-1 Degradation and mRNA Downregulation and Myofibroblast Differentiation in Cultured Human Dental Pulp Tissue. J Histochem Cytochem 2015;63(6):438–48. Doi: 10.1369/0022155415580622.
13. Duijvestijn AM, van Goor H, Klatter F, Majoor GD, van Bussel E, van Breda Vriesman PJ. Antibodies defining rat endothelial cells: RECA-1, a pan-endothelial cell-specific monoclonal

antibody. Lab Invest 1992;66(4):459–66.

14. Stallcup WB. The NG2 proteoglycan: Past insights and future prospects. J Neurocytol 2002;31(6–7):423–35. Doi: 10.1023/A:1025731428581.
15. Moore-morris T, Guimarães-camboa N, Banerjee I, et al. Resident fibroblast lineages mediate pressure overload-induced cardiac fibrosis. J Clin Invest 2014;124(7):1–14. Doi: 10.1172/JCI74783.
16. Tomasek JJ, Gabbiani G, Hinz B, Chaponnier C, Brown RA. Myofibroblasts and mechano-regulation of connective tissue remodelling. Nat Rev Mol Cell Biol 2002;3(5):349–63. Doi: 10.1038/nrm809.
17. Bhattacharyya S, Tamaki Z, Wang W, et al. FibronectinEDA Promotes Chronic Cutaneous Fibrosis Through Toll-Like Receptor Signaling. Sci Transl Med 2014;6(232):232ra50-232ra50. Doi: 10.1126/scitranslmed.3008264.20
18. Wynn TA. Cellular and molecular mechanisms of fibrosis. J Pathol 2008;214(2):199–210. Doi: 10.1002/path.2277.
19. Melin M, Joffre-Romeas A, Farges JC, Couble ML, Magloire H, Bleicher F. Effects of TGFbeta1 on dental pulp cells in cultured human tooth slices. J Dent Res 2000;79(9):1689–96.
20. Hirata A, Dimitrova-Nakov S, Djole SX, et al. Plithotaxis, a collective cell migration, regulates the sliding of proliferating pulp cells located in the apical niche. Connect Tissue Res 2014;55 Suppl 1(3):68–72. Doi: 10.3109/03008207.2014.923855.
21. Zhu L, Yang J, Zhang J, Peng Bin. A comparative study of bioaggregate and ProRoot MTA on adhesion, migration, and attachment of human dental pulp cells. J Endod 2014;40(8):1118–23. Doi: 10.1016/j.joen.2013.12.028.
22. Hinz B, Phan SH, Thannickal VJ, et al. Recent developments in myofibroblast biology: Paradigms for connective tissue remodeling. Am J Pathol 2012;180(4):1340–55. Doi: 10.1016/j.ajpath.2012.02.004.
23. Kramann R, Schneider RK, Dirocco DP, et al. Perivascular Gli1+ progenitors are key contributors to injury-induced organ fibrosis. Cell Stem Cell 2015;16(1):51–66. Doi: 10.1016/j.stem.2014.11.004.
24. Zhao H, Feng J, Seidel K, et al. Secretion of Shh by a Neurovascular Bundle Niche Supports Mesenchymal Stem Cell Homeostasis in the Adult Mouse Incisor. Cell Stem Cell 2014;14(2):160–73. Doi: 10.1016/j.stem.2013.12.013.
25. Menard C, Mitchell S, Spector M. Contractile behavior of smooth muscle actin-containing osteoblasts in collagen-GAG matrices in vitro: implant-related cell contraction. Biomaterials 2000;21(18):1867–77.
26. Hosoya A, Yukita A, Yoshiba K, Yoshiba N, Takahashi M, Nakamura H. Two Distinct Processes of Bone-like Tissue Formation by Dental Pulp Cells after Tooth Transplantation. J Histochem

Cytochem 2012;60(11):861–73. Doi: 10.1369/0022155412459741.

27. Vidovic I, Banerjee A, Fatahi R, et al. αSMA-Expressing Perivascular Cells Represent Dental Pulp Progenitors In Vivo. J Dent Res 2016. Doi: 10.1177/0022034516678208.

Figure legends

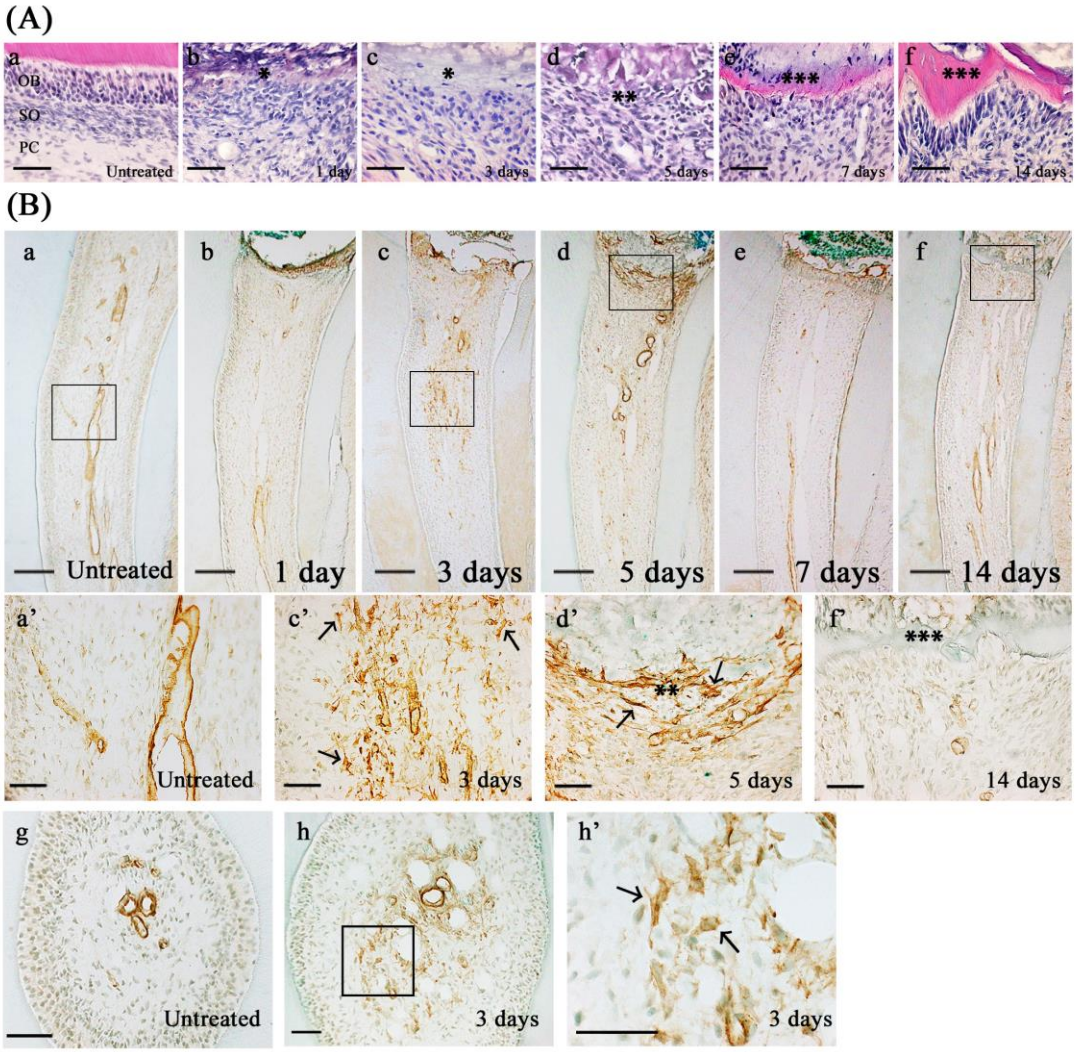

Figure 1. Histological alteration, and immunohistochemical staining for α-SMA during wound healing after pulpotomy with MTA. Hematoxylin-eosin staining (A), immunostaining for α-SMA (B). Higher magnification views of the boxed areas in (B a, c, d, f, h) are shown in (B a', c', d', f', h'), respectively, in sagittal (B a–f) and horizontal (B g–h) sections. Immunoreactivity for α-SMA is detectable in spindle-shaped cells in the pulp core at 3 days and at the amputated site at 5 days (B c', d', h', arrows). OB, odontoblast layer; SO, sub-odontoblastic layer; PC, Pulp core; *, degenerative layer; **, granulation-like tissue; ***, dentin bridge. Scale 200 μm (B a–f); 50 μm (A) (B a' c' d' f' g h h').

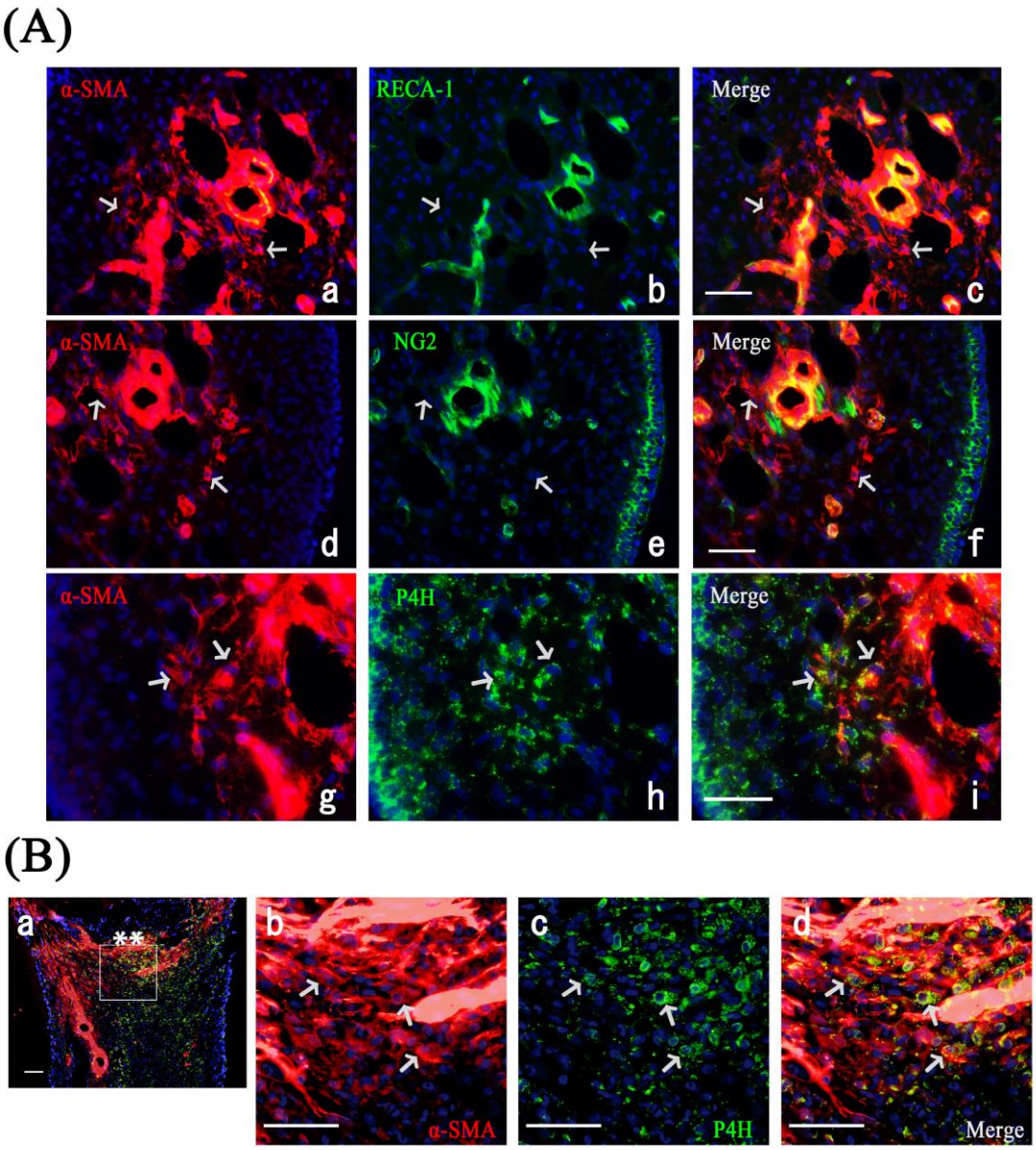

Figure 2. Double-labeling immunofluorescence for α-SMA and RECA-1, NG2, or P4H during wound healing after pulpotomy with MTA. All images in **A** are horizontal sections at 3 days and those in **B** are sagittal sections at 5 days. Higher magnification views of the boxed areas in (B a) are shown in (B b–d) α-SMA-positive spindle-shaped cells, which are isolated from RECA-1 positive cells, are present in the pulp core at 3 days (A a–c, arrows). These α-SMA-positive spindle-shaped cells do not express NG2 (A d–f, arrows) but do express P4H (A g–i, arrows). α-SMA-positive spindle-shaped cells co-express P4H at 5 days as well (B b–d, arrows). Nuclei (DAPI, blue). **, granulation-like tissue. Scale 50 μm.

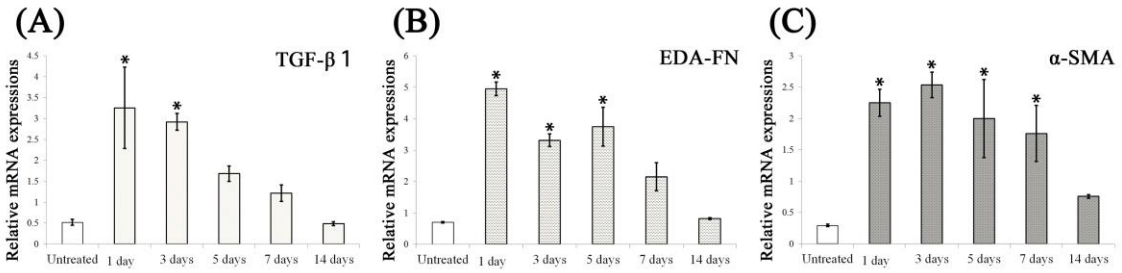

Figure 3. Quantitative RT-PCR analysis of TGF-β1 (A), EDA-FN (B), and α-SMA (C). Bars represent mean values ± standard error of the mean (n = 4). *Significant difference compared with untreated normal, $p < 0.05$.

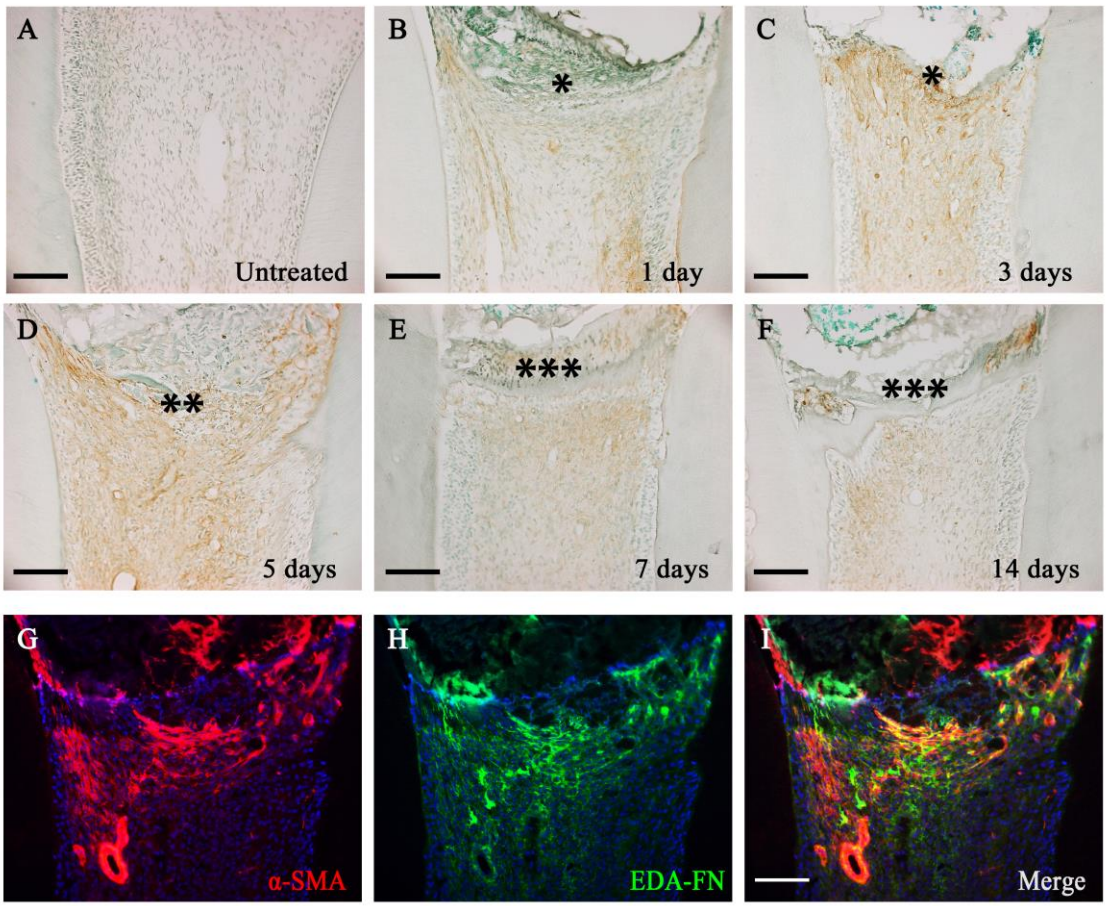

Figure 4. Immunohistochemical staining of EDA-FN and double immunofluorescence for α-SMA and EDA-FN in the process of wound healing after pulpotomy with MTA. The distribution of accumulated α-SMA positive cells overlaps with the strong EDA-FN immunofluorescence at the exposure site at 5 days (G–I). *, degenerative layer; **, granulation-like tissue; ***, dentin bridge. Scale 100 μm.

Table 1. Primary Antibodies Used in This Study

Antibody	Clone	Source
mouse anti-α-SMA	1A4	Sigma-Aldrich, St Louis, MO, USA
Cy3-conjugated mouse anti-α-SMA	1A4	Sigma-Aldrich, St Louis, MO, USA
mouse anti-RECA-1	HIS52	AbD Serotec, Oxford, UK
rabbit anti-NG2	polyclonal	Chemicon, Temecula, CA, USA
mouse anti-P4H	6-9H6	Acris Antibodies, Herford, DE
mouse anti-EDA-FN	DH1	Chemicon, Temecula, CA, USA

α-SMA: alpha smooth muscle actin; P4H: Prolyl-4-hydroxylase; EDA-FN: extradomain A fibronectin splice variant

Table 2. Primers Used in This Study

			Primer	
Molecular name	Accession no.	Name of oligomer	Sequence	Expected size (bp)
α-SMA	NM_031004.2	Sence primer	CAGGGAGTGATGGTTGGAATG	113
		Anti-sence primer	TTGGTGATGATGCCGTGTTC	
TGF-β1	NM_021578.2	Sence primer	CAATTCCTGGCGTTACCTTG	123
		Anti-sence primer	AAGCCCTGTATTCCGTCTCC	
EDA-FN	NM_019143.1	Sence primer	GACTGTGTACTCAGAACCCG	116
		Anti-sence primer	ACAGGGTGACCTACTCAAGC	
β-actin	NM_031144.2	Sence primer	CAGGGTGTGATGGTGGGTAT	146
		Anti-sence primer	GTGTGGTGCCAAATCTTCTC	

α-SMA: alpha smooth muscle actin; TGF-β1; transforming growth factor-β1 ; EDA-FN: extradomain A fibronectin splice variant